Nuclear Engineering and Technology 53 (2021) 142–147

Contents lists available at ScienceDirect

Nuclear Engineering and Technology

journal homepage: www.elsevier.com/locate/net

Original Article

An electrochemical hydrogen peroxide sensor for applications in nuclear industry

Junghwan Park [a, b, *], Jong Woo Kim [c], Hyunjin Kim [d], Wonhyuck Yoon [e]

[a] Nuclear Chemistry Research Team, Korea Atomic Energy Research Institute, 111, Daedeok-daero, 989 Beon-gil, Yuseong-gu, Daejeon, 34057, Republic of Korea
[b] Department of Nuclear and Quantum Engineering, Korea Advanced Institute of Science and Technology, 291 Daehak-ro, Yuseong-gu, Daejeon, 34141, Republic of Korea
[c] Engineering Development Research Center, Seoul National University, 1, Gwanak-ro, Gwanak-gu, Seoul, 08826, Republic of Korea
[d] College of Pharmacy, Seoul National University, 1, Gwanak-ro, Gwanak-gu, Seoul, 08826, Republic of Korea
[e] School of Mechanical and Aerospace Engineering, Seoul National University, 1, Gwanak-ro, Gwanak-gu, Seoul, 08826, Republic of Korea

ARTICLE INFO

Article history:
Received 7 May 2020
Received in revised form
15 June 2020
Accepted 27 June 2020
Available online 27 July 2020

Keywords:
Hydrogen peroxide
Coolant chemistry
Radiolysis
Spent fuel
Sensor

ABSTRACT

Hydrogen peroxide is a radiolysis product of water formed under gamma-irradiation; therefore, its reliable detection is crucial in the nuclear industry for spent fuel management and coolant chemistry. This study proposes an electrochemical sensor for hydrogen peroxide detection. Cysteamine (CYST), gold nanoparticles (GNPs), and horseradish peroxidase (HRP) were used in the modification of a gold electrode for fabricating Au/CYST/GNP/HRP sensor. Each modification step of the electrode was investigated through electrochemical and physical methods. The sensor exhibited strong sensitivity and stability for the detection and measurement of hydrogen peroxide with a linear range of 1–9 mM. In addition, the Michaelis–Menten kinetic equation was applied to predict the reaction curve, and a quantitative method to define the dynamic range is suggested. The sensor is highly sensitive to H_2O_2 and can be applied as an electrochemical H_2O_2-sensor in the nuclear industry.

1. Introduction

Hydrogen peroxide (H_2O_2) is a highly interesting topic in the nuclear industry. H_2O_2 is generated during the radiolysis of water, and is a typical oxidant [1–6]. The radiolysis of water can be as described as the following reaction:

$$H_2O \xrightarrow{Ionizing\ Radiation} H_2 + H_2O_2 + H\bullet + HO\bullet + HO_2\bullet + e_{aq}.$$

H_2O_2 has been extensively used in several critical applications in various avenues of nuclear science and technology. For example, water is used as a coolant in commercial nuclear reactors, such as pressurized water reactors and boiling water reactors. Therefore, water radiolysis and H_2O_2-related chemistry are relevant to the coolant attributes of water. In addition, H_2O_2 is employed for cleaning the steam generators of the primary nuclear reactor coolant [7–10] and as a decontaminant in the reactor shutdown process [11,12]. During the storage of spent nuclear fuel in underground repositories, the radiolysis of the underground water can affect the long-term safety of the copper-steel containers that are used for the storage of the nuclear fuel due to the formation of H_2O_2 [13–19]. Furthermore, the spent fuel itself is exposed to oxidizing conditions caused by its alpha-radiolysis [20–22], which could compromise its surface integrity. Due to these reasons, the detection and measurement of H_2O_2 are crucial in the nuclear industry. However, to the best of our knowledge, there are no standard methods for real-time monitoring H_2O_2, that can be used for practical applications in the nuclear industry.

The aim of this study is the development, production, and qualification of an electrochemical sensor for the specific detection of H_2O_2, using novel materials, for improving operational safety in the nuclear industry. Gold nanoparticles (GNPs) afford a uniquely fast electron transport rate, which is referred to as an 'electron antenna' [23], and they can fabricated onto the functional groups of organic materials owing to their large surface area [24,25]. By merging the beneficial properties of gold nanoparticles and an enzyme that can catalyze the reduction of H_2O_2, an electrochemical sensor with high sensitivity and selectivity for H_2O_2-detection can be engineered.

* Corresponding author. Nuclear Chemistry Research Team, Korea Atomic Energy Research Institute, 111, Daedeok-daero, 989 beon-gil, Yuseong-gu, Daejeon, 34057, Republic of Korea.
E-mail address: jpark7@kaeri.re.kr (J. Park).

https://doi.org/10.1016/j.net.2020.06.031

Recently, electrochemical sensors based on metal nanoparticles and enzymes have been actively researched for application to hydrogen peroxide detection in various fields, including food, pharmaceutical, medicinal, and environmental industries [26,27], and could also be employed for applications in the nuclear industry. For such a development of H_2O_2 sensors [20,28–31], the horseradish peroxidase (HRP) enzymes were chosen from the family of redox enzymes and were fabricated along with GNPs on the electrode surface. HRP, as its nomenclature refers, is an H_2O_2 redox enzyme, and its catalytic active site is referred to as a prosthetic group [32,33]. Importantly, HRP is estimated to detect and measure hydrogen peroxide selectively, and its performance, including efficiency, detection range, and detection limit, can be improved [31,34].

In this work, an electrochemical sensor was prepared by reforming a gold (Au) electrode surface with a cysteamine (CYST) self-assembled monolayer, which is an organic material that assists the fabrication of the GNPs on the Au electrode. The Au/CYST/GNP electrode was prepared by the chemical adsorption of gold nanoparticles on the Au/CYST electrode surface. Next, the immobilization of the HRP on the nanoparticles was carried out for the preparation of the Au/CYST/GNP/HRP electrode, which completed the fabrication of the electrochemical sensor. The electrode modifications in each step were qualified using electrochemical and physical methods. The developed sensor had high sensitivity and stability toward H_2O_2. The performance of the sensor was assessed using electrochemical methods. In addition, the Michaelis–Menten (K_m) constant and the affinity of HRP to H_2O_2 were evaluated using the Michaelis–Menten kinetic equation and Lineweaver–Burk equation [35,36]. The cathodic current over the range beyond the one measured is estimated using the Michaelis–Menten kinetic equation, and a dynamic range of the sensor is suggested.

2. Materials and methods

2.1. Chemicals and apparatus

HRP (250 U/mg, RZ $\geq$ 2.0, Sigma, USA), $HAuCl_4$ (Au $\geq$ 49%, ACROS organics, USA), and cystamine (95%, Sigma, USA) were employed for electrode modification. Potassium ferricyanide (99%, Sigma, USA), Dopamine (98%, Acros, USA), L-ascorbic acid (99%, Sigma, USA), and hydrogen peroxide (30 wt% in H_2O, Sigma, USA) were used for the preparation of the analytes. All other chemicals were of analytical grade and purchased from Sigma and used without further purification. All solutions were prepared using water purified by reverse osmosis and electrodeionization (Milli Q academic, Merck, USA). Potassium phosphate and potassium dihydrogen phosphate were used for the preparation of 0.1 M, pH 7 phosphate buffer solution (PBS). Unless specified otherwise, all experiments were carried out at 25 °C.

Electrochemical measurements were performed with a potentiostat (CHI440, CH Instruments, USA). The three-electrode system consisted of an Au electrode as the working electrode, a Pt electrode as the counter electrode, and a saturated Ag/AgCl electrode as the reference electrode. The working electrode was polished with alumina powder (1.0, 0.3, and 0.05 μm) on silica pads and sonicated in water, ethanol, and water for 10 min each, in that order. The working electrode was then cleaned electrochemically in sulfuric acid by cyclic voltammetry in the 1.5 to −0.2 V range with a scan rate of 300 mV/s. Scanning electron microscope (SEM, S-4800, Hitachi, Japan) was used for observing the Au colloids.

2.2. Preparation of Au/CYST/GNP electrode

The Au electrode was qualified using a ferricyanide solution. The qualified Au electrode was immersed for 1 h in a 10 mM solution of CYST in PBS at 4 °C for preparing the Au/CYST electrode. The Au colloids were prepared according to a reported procedure [23,37,38]. A solution of 1 mL of 1% $HAuCl_4$ and 90 ml of H_2O was prepared by stirring for 1 min. To prepare the spherical-shaped colloidal form, 38.8 ml of sodium citrate was added, and then 1 ml of 0.075% sodium borohydride was used for the reduction and shaping of the Au colloids. Once the solution turned burgundy, it was stirred for 10 min without heating. The concentration of the Au colloids was estimated to be 0.32 μM [23,39]. Finally, the prepared Au/CYST electrode was immersed in the Au colloids at 4 °C for 12 h in the absence of light. The adsorption of the Au colloids on the electrode as GNPs completed the fabrication of the Au/CYST/GNP electrode. To validate the electrode, a solution of dopamine (DA) and L-ascorbic acid (AA) was prepared in PBS. Square wave voltammetry (SWV) was performed with solutions of various concentrations to test the electrode by comparison with a reported study [23].

2.3. Preparation of Au/CYST/GNP/HRP and H_2O_2 detection

HRP (15 mg) was dissolved in 5 mL of PBS and stirred for 10 min. Then, the Au/CYST/GNP electrode was immersed in the HRP PBS solution at 4 °C for 12 h. CV was performed with 1 mM H_2O_2 in PBS with a scan rate of 100 mV/s and a range from −0.7 to 0.4 V. The optimal reduction potential was determined to be −0.3 V, which was then applied to amperometry. The amperometry was performed for various concentrations of H_2O_2 in 5 mL PBS were measured for 100 s at a scan-interval of 0.1 s in a cell. The cell was stirred continuously to maintain a homogenous solution.

3. Results and discussion

3.1. Modification of Au/CYST/GNP/HRP

Cyclic voltammetry of $Fe(CN)_6^{3-}$ in PBS was carried out at different concentrations, with the Au electrode at a scan rate of 100 mV/s (Fig. 1 (a)). The redox reaction of $Fe(CN)_6^{3-}$ is a well-known redox process at the Au electrode [40]. Since the redox of ferricyanide is a simple electron transfer reaction without a side reaction and the electrochemical reaction is easily processed, it is simple to test the electrode without further modification of the electrochemical cell system. The peak currents of the cathodic wave and the cathodic current of each cycle were obtained and linearly regressed, as shown in Fig. 1 (b). The cathodic current was linearly dependent on the concentration of ferricyanide, which indicated that the Au electrode component of the electrochemical sensor was appropriately prepared.

The colloidal Au solution was visually inspected using SEM with a magnification of 100 000 at 15.0 kV. The colloids were uniformly produced in the spherical form, with sizes ranging from 20 to 30 nm, as seen in Fig. 2. After CYST was self-assembled and immobilized on the Au electrode, the Au colloids were added to the Au/CYST electrode as gold nanoparticles. Performance testing of the Au/CYST/GNP using SWV was carried out with a mixed solution of AA and DA in PBS, at various concentrations. SWV was performed with a scan increment of 0.004 V, amplitude of 0.025 V, and frequency of 15 Hz. The results are shown in Fig. 3 (a) and indicate two remarkable peaks at 0 and 0.2 V. The peaks at 0 and 0.2 V have been reported to be attributable to the oxidation potentials of AA and DA, respectively [23]. The peak currents of AA and DA, as anodic currents over each concentration, were linearly regressed, and the results are shown in Fig. 3 (b). The results indicate good sensitivity for the separation of the voltammetric signals of AA and DA, which confirms that the prepared Au/CYST/GNP electrode operated suitably [23]. As a consequence, Au/CYST/GNP electrode was qualified.

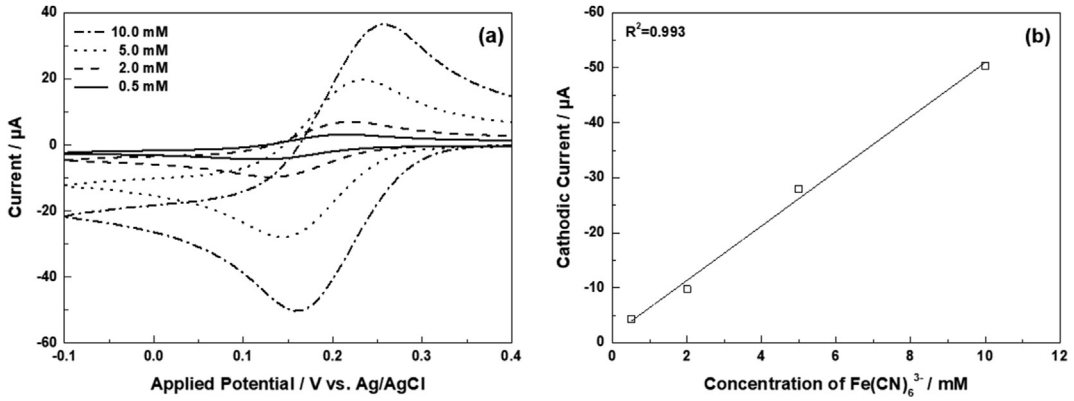

Fig. 1. (a) CV of ferricyanide in pH 7 PBS at 25 °C on Au electrode with scan rate of 100 mV/s and (b) cathodic current of ferricyanide reduction over various concentrations.

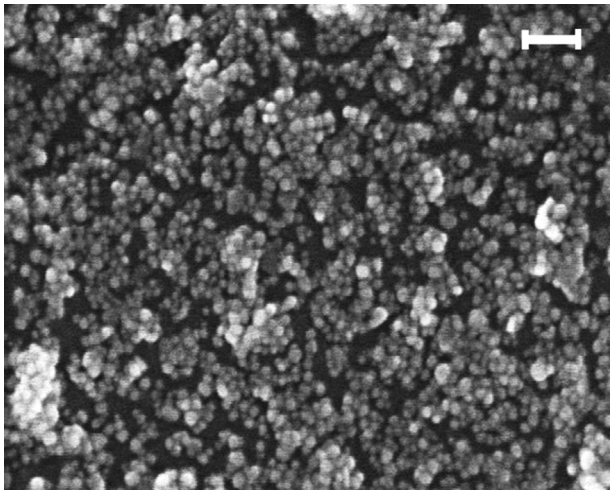

Fig. 2. Microscopic image, with a 100 nm white bar, for SEM of Au colloids at 100 000 magnification.

After immobilization of HRP on the Au/CYST/GNP electrode, the resulting Au/CYST/GNP/HRP electrode was fabricated, as shown in Fig. 4. CV of the electrode was performed with a scan rate of 100 mV/s in PBS, and 1 mM H_2O_2 in PBS, as shown in Fig. 5. At −0.3 V, the cathodic wave of H_2O_2 began to show distinction from the cathodic wave of PBS, which was used as the background signal. This result indicates that the H_2O_2 underwent a reduction reaction at the prosthetic group of HRP [32,33] and degraded into H_2O and O_2 [32,41,42] (Fig. 6). Electrochemical investigations of the properties of H_2O_2, with pH control [43], have indicated that the reduction potential of H_2O_2 is −0.3 V in the middle of the diffusion-controlled region, at pH 7 and 25 °C. Although the cathodic current with a lower reduction potential is more distinct between H_2O_2 and PBS, it is estimated that there would be some side reactions, such as hydrogen production, which could interrupt the current signal [43]. Therefore, it was concluded that −0.3 V is the optimal potential for the electrochemical detection of H_2O_2 reduction in the current system.

3.2. H_2O_2 detection and measurement

The quantitation of the H_2O_2 reduction with the Au/CYST/GNP/HRP electrode was carried out using amperometry. Samples with various concentrations (1, 2, 3, 4, 5, 6, 7, 8, and 9 mM) of H_2O_2 in PBS were measured for 100 s at a scan-interval of 0.1 s. The background signal was obtained from PBS. The cathodic current at each concentration is shown in Fig. 7. The current obtained was linearly dependent on the concentration in the 1–9 mM range, which indicates that the Au/CYST/GNP/HRP electrochemical sensor is strongly sensitive to H_2O_2. From the standard deviation of the background amperometric current in PBS and the slope (Fig. 7), the limit of detection (LOD) [44] was determined to be 0.12 mM.

It has been reported that the concentration of H_2O_2 has been measured up to the mM scale in the coolant chemistry [3] and that of spent fuel [20]. Also, 8.8 mM H_2O_2 was used in the chemical and

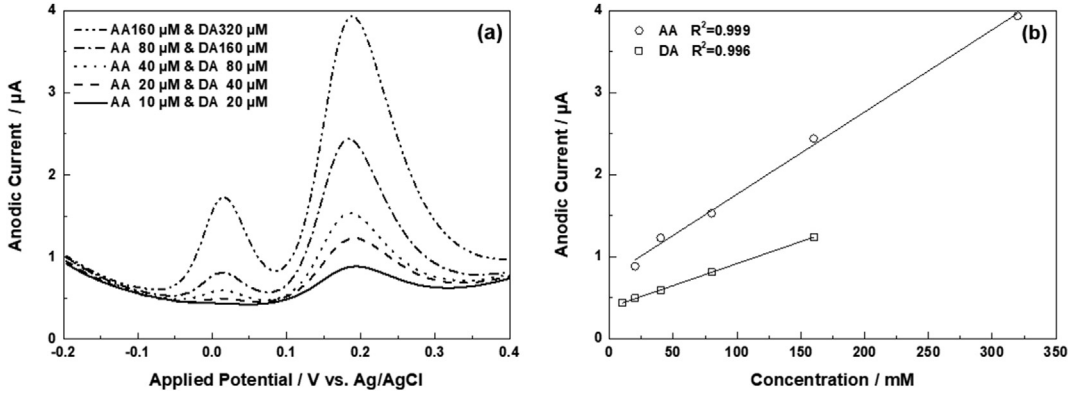

Fig. 3. (a) SWV of AA and DA mixture in pH 7 PBS at 25 °C on Au/CYST/GNP electrode with scan increments of 0.004 V, amplitude of 0.025 V, and frequency of 15 Hz and (b) anodic current of AA and DA at various concentrations.

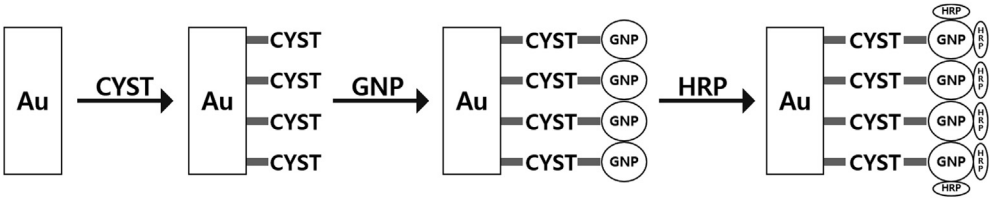

Fig. 4. Modification process of Au/CYST/GNP/HRP electrode.

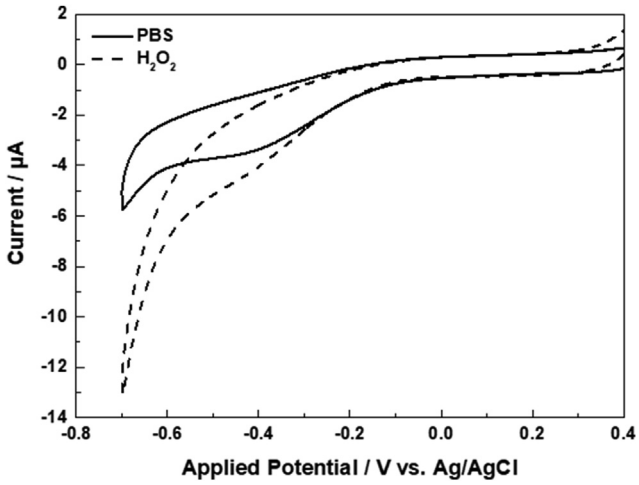

Fig. 5. CV of 1 mM H_2O_2 in pH 7 PBS at 25 °C on Au/CYST/GNP/HRP electrode with scan rate of 100 mV/s.

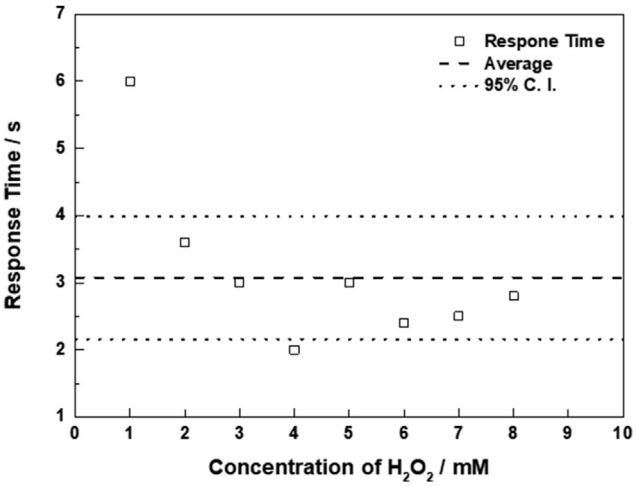

Fig. 8. Response time of amperometry of H_2O_2 reduction over various concentrations, in pH 7 PBS at 25 °C on Au/CYST/GNP/HRP electrode.

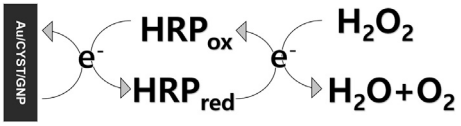

Fig. 6. Electron transfer and redox mechanism on Au/CYST/GNP/HRP electrode.

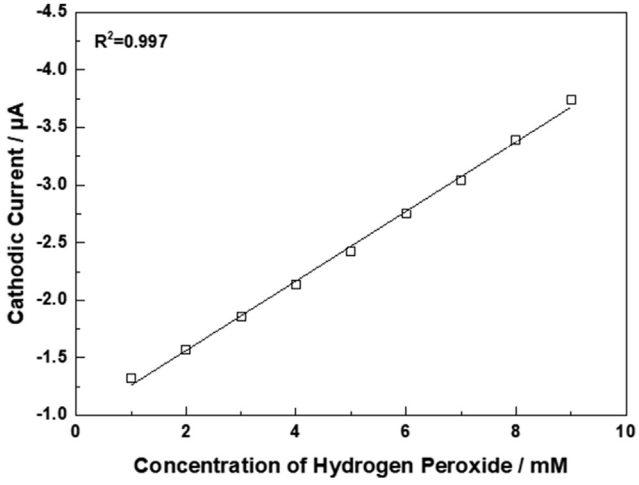

Fig. 7. Cathodic current from H_2O_2 reduction over various concentrations, in pH 7 PBS at 25 °C on Au/CYST/GNP/HRP electrode.

volume control system of a commercial reactor according to a US Nuclear Regulatory Commission report [45], and the oxidative dissolution of the spent fuel appears to range from 0.1 to 5.0 mM [21]. Therefore, the linear range of our sensor, meets significantly, the requirements of the nuclear industry for H_2O_2 detection. Therefore, the linear range of the proposed sensor meets the requirements of the nuclear industry for H_2O_2 detection. Since there is no direct method to measure H_2O_2 and the estimation method uses electrochemical corrosion potential only [3], this work can be applied as a direct measurement.

Response time is another vital attribute of sensors [46]. In this case, the response time can be defined as the time at which a steep interval signal is obtained after the commencement of the measurement. Such a signal was obtained during the amperometry at each concentration (Fig. 8), with an average value of 3.1 s and a 95% confidence interval. Except for the initial point, all other data were uniformly distributed. As the response time increased, the current signal remained constant, which indicates that the electrode is highly stable to concentration changes over time and that the structure of the electrode inhibits the enzyme denaturation [33].

3.3. Michaelis–Menten kinetics

As HRP is a biochemical enzyme, it follows the Michaelis–Menten kinetic equation. The Michaelis–Menten constant (K_m) can be acquired using the correlation between the concentration and the current [32,35,47]. K_m is identical to the concentration at the half-maximum reaction rate, and therefore, an inverse indicator of the affinity between the substrate and the enzyme [35,48]. Because K_m cannot be directly evaluated from the equation, the Lineweaver–Burk equation can be used instead to calculate K_m, according to the following equation [30,33,36,49]:

$$\frac{1}{I}=\frac{K_m}{I_{max}}\frac{1}{C}+\frac{1}{I_{max}}. \quad (1)$$

Equation (1) is an alternate expression of the Lineweaver–Burk equation, which can be applied for electrochemical reactions, where I and I_{max} are the currents detected under the steady-state and saturated conditions, respectively, and C is the concentration of the analyte [50]. In this case, I is the cathodic current, and C is the concentration of H_2O_2 from amperometry. The plots for the inverse cathodic current and inverse concentration of H_2O_2 are shown in Fig. 9. From the slope, K_m/I_{max}, and the intercept $1/I_{max}$ of the Lineweaver–Burk plot, the K_m was determined to be 6.3 mM. The Michaelis–Menten equation for the electrochemical reaction from equation (1) can be expressed as follows:

$$I=\frac{I_{max}C}{K_m+C}. \quad (2)$$

Using equation (2), the current was estimated and plotted over the concentration beyond the range measured, as shown in Fig. 10. The slope of the plot in Fig. 7 was extrapolated to determine the maximum current I_{max}, which was determined to be at a concentration of 15.6 mM. Although the range from 1 to 15.6 mM was not linear, it could be treated as a dynamic range, where the data are nonlinear, but measurable [44]. Dynamic ranges are observed in a wide range of experiments and are typically determined intuitively. Therefore, such dynamic ranges are inconvenient and typically avoided. Wider ranges can be estimated using the Michaelis–Menten kinetic equation, even with smaller data, and the dynamic range suggested above is more quantitative. However, the denaturation of HRP has been reported at higher concentrations of H_2O_2 [31,32], and further research is needed to confirm the stability in the wider ranges of concentration. Also, effect of radiation on the sensor in a more specific condition should be studied in the future.

4. Conclusion

This study reports the successful fabrication of a novel Au/CYST/GNP/HRP electrode, which was qualified experimentally and by examination using SEM image at each modification step of the Au electrode. The performance of the sensor was tested, and the sensitivity and LOD were evaluated. The electrochemical sensor was stable to concentration changes and did not exhibit any deformation. The optimal conditions for the diffusion-controlled reaction at the sensor were determined. The cathodic current of the sensor in the range beyond the one measured was estimated using the Michaelis–Menten kinetic equation, and a quantitative definition of the dynamic range is suggested. The sensor is highly sensitive to H_2O_2 and can be applied as an electrochemical H_2O_2-sensor in the nuclear industry including coolant chemistry and spent fuel management in the terms of nuclear safety.

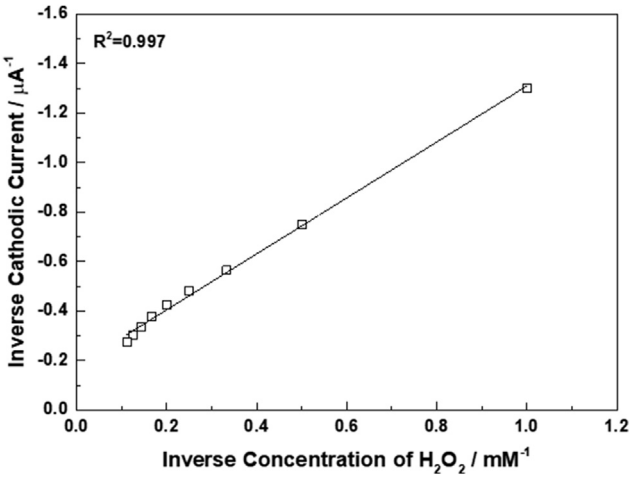

Fig. 9. Inverse cathodic current of H_2O_2 reduction over its inverse concentration, in pH 7 PBS at 25 °C on Au/CYST/GNP/HRP electrode.

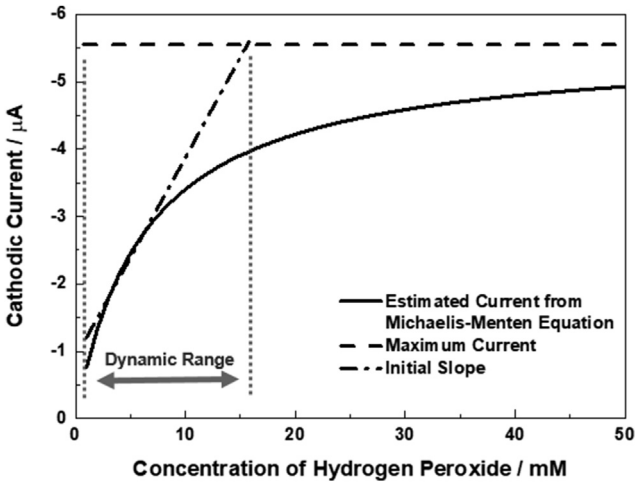

Fig. 10. Estimated cathodic current with Michaelis–Menten equation beyond the range measured, for H_2O_2 reduction over various concentrations, in pH 7 PBS at 25 °C on Au/CYST/GNP/HRP electrode, with an extended initial slope of linear range from Fig. 7 and dynamic range, suggested in this study.

Declaration of Competing Interest

The authors declare that they have no known competing financial interests or personal relationships that could have appeared to influence the work reported in this paper.

Acknowledgements

This research was supported by the National Research Foundation of Korea (NRF) funded by Korean government (Ministry of Science and ICT) (Grant No. 2017M2A8A5014754).

References

[1] H. Christensen, Remodeling of the oxidant species during radiolysis of high-temperature water in a pressurized water reactor, Nucl. Technol. 109 (1995) 373–382, https://doi.org/10.13182/NT95-A35086.
[2] B. Pastina, J.A. LaVerne, Effect of molecular hydrogen on hydrogen peroxide in water radiolysis, J. Phys. Chem. 105 (2001) 9316–9322, https://doi.org/10.1021/jp012245j.
[3] H. Takiguchi, M. Ullberg, S. Uchida, Optimization of dissolved hydrogen concentration for control of primary coolant radiolysis in pressurized water reactors, J. Nucl. Sci. Technol. 41 (2004) 601–609, https://doi.org/10.1080/18811248.2004.9715523.
[4] J.C. Wren, Steady-state radiolysis: effects of dissolved additives, in: Nucl. Energy Environ., American Chemical Society, 2010, pp. 22–271, https://doi.org/10.1021/bk-2010-1046.ch022.
[5] Y. Kumagai, A. Kimura, M. Taguchi, R. Nagaishi, I. Yamagishi, T. Kimura, Hydrogen production in gamma radiolysis of the mixture of mordenite and seawater, J. Nucl. Sci. Technol. 50 (2013) 130–138, https://doi.org/10.1080/00223131.2013.757453.
[6] K. Hata, H. Inoue, T. Kojima, A. Iwase, S. Kasahara, S. Hanawa, F. Ueno, T. Tsukada, Hydrogen peroxide production by gamma radiolysis of sodium chloride solutions containing a small amount of bromide ion, Nucl. Technol. 193 (2016) 434–443, https://doi.org/10.13182/NT15-32.
[7] A. Rufus, V. Sathyaseelan, M. Srinivasan, P.S. Kumar, S. Veena, S. Velmurugan, S. Narasimhan, Chemistry aspects pertaining to the application of steam generator chemical cleaning formulation based on ethylene diamine tetra acetic acid, Prog. Nucl. Energy 39 (2001) 285–303, https://doi.org/10.1016/S0149-1970(01)00004-X.

[8] H. Kawamura, K. Fujiwara, H. Kanbe, H. Hirano, H. Takiguchi, K. Yoshino, S. Yamamoto, T. Shibata, K. Ishigure, Applicability of chemical cleaning process to steam generator secondary side, (III), J. Nucl. Sci. Technol. 43 (2006) 655–668, https://doi.org/10.1080/18811248.2006.9711145.

[9] M. Suzuki, E. Oohashi, Cleaning the secondary side of steam generators of Tomari Power Station Unit 1/2 using ASCA and UEC technology, E-Journal Adv. Maint. 4 (2012) 7. http://inis.iaea.org/search/search.aspx?orig_q=RN:44084602.

[10] S. Uchida, Y. Katsumura, Water chemistry technology – one of the key technologies for safe and reliable nuclear power plant operation, J. Nucl. Sci. Technol. 50 (2013) 346–362, https://doi.org/10.1080/00223131.2013.773171.

[11] J.W. Kormuth, The control of cobalt-58 dissolution during refueling shutdowns of pressurized water reactors using a hydrogen peroxide addition, Nucl. Technol. 37 (1978) 99–102, https://doi.org/10.13182/NT78-A31976.

[12] I. Betova, M. Bojinov, T. Saario, Start-up and shut-down water chemistries in pressurized water reactors, VTT Res. Rep. (2012) 1–81. VTT-R-00699-12, http://www.vtt.fi/inf/julkaisut/muut/2012/VTT-R-00699-12.pdf.

[13] J.P. Simpson, P.H. Valloton, Experiments on Container Materials for Swiss High-Level Waste Disposal Projects Part II, Nagra NTB, 1984, pp. 1–84.

[14] W.H. Yunker, R.S. Glass, Long-term corrosion behavior of copper-base materials in a gamma-irradiated environment, MRS Proc. 84 (1986) 579, https://doi.org/10.1557/PROC-84-579.

[15] F. King, C.D. Litke, The Corrosion of Copper in Synthetic Groundwater at 150 C-Part I. The Results of Short-Term Electrochemical Tests, 1987.

[16] J. Kass, Evaluation of copper, aluminum bronze, and copper-nickel container material for the Yucca mountain project, Canada. http://inis.iaea.org/search/search.aspx?orig_q=RN:23004457, 1990.

[17] C. Corbel, V. Wasselin-Trupin, B. Hickel, D. Feron, M. Roy, F. Maurel, Effect of irradiation on long term alteration of oxides and metals in aqueous solutions. https://inis.iaea.org/search/search.aspx?orig_q=RN:35038877, 2003 (accessed April 10, 2020).

[18] Å. Björkbacka, S. Hosseinpour, C. Leygraf, M. Jonsson, Radiation induced corrosion of copper in anoxic aqueous solution, Electrochem. Solid State Lett. 15 (2012), https://doi.org/10.1149/2.022205esl.

[19] Å. Björkbacka, S. Hosseinpour, M. Johnson, C. Leygraf, M. Jonsson, Radiation induced corrosion of copper for spent nuclear fuel storage, Radiat. Phys. Chem. 92 (2013) 80–86, https://doi.org/10.1016/J.RADPHYSCHEM.2013.06.033.

[20] G. Sattonnay, C. Ardois, C. Corbel, J.F. Lucchini, M.-F. Barthe, F. Garrido, D. Gosset, Alpha-radiolysis effects on UO2 alteration in water, J. Nucl. Mater. 288 (2001) 11–19, https://doi.org/10.1016/S0022-3115(00)00714-5.

[21] E. Ekeroth, M. Jonsson, Oxidation of UO_2 by radiolytic oxidants, J. Nucl. Mater. 322 (2003) 242–248, https://doi.org/10.1016/J.JNUCMAT.2003.07.001.

[22] E. Ekeroth, O. Roth, M. Jonsson, The relative impact of radiolysis products in radiation induced oxidative dissolution of UO_2, J. Nucl. Mater. 355 (2006) 38–46, https://doi.org/10.1016/J.JNUCMAT.2006.04.001.

[23] C.R. Raj, T. Okajima, T. Ohsaka, Gold nanoparticle arrays for the voltammetric sensing of dopamine, J. Electroanal. Chem. 543 (2003) 127–133, https://doi.org/10.1016/S0022-0728(02)01481-X.

[24] A.N. Shipway, E. Katz, I. Willner, Nanoparticle arrays on surfaces for electronic, optical, and sensor applications, ChemPhysChem 1 (2000) 18–52, https://doi.org/10.1002/1439-7641(20000804)1:1<18::AID-CPHC18>3.0.CO;2-L.

[25] T. Sagara, N. Kato, N. Nakashima, Electroreflectance study of gold nanoparticles immobilized on an aminoalkanethiol monolayer coated on a polycrystalline gold electrode surface, J. Phys. Chem. B 106 (2002) 1205–1212, https://doi.org/10.1021/jp011807w.

[26] J. Wang, Y. Lin, L. Chen, Organic-phase biosensors for monitoring phenol and hydrogen peroxide in pharmaceutical antibacterial products, Analyst 118 (1993) 277–280, https://doi.org/10.1039/AN9931800277.

[27] M. Shamsipur, M. Asgari, M.G. Maragheh, A.A. Moosavi-Movahedi, A novel impedimetric nanobiosensor for low level determination of hydrogen peroxide based on biocatalysis of catalase, Bioelectrochemistry 83 (2012) 31–37, https://doi.org/10.1016/J.BIOELECHEM.2011.08.003.

[28] P.D. Sánchez, P.T. Blanco, J.M.F. Alvarez, M.R. Smyth, R. O'Kennedy, Flow-injection analysis of hydrogen peroxide using a horseradish peroxidase-modified electrode detection system, Electroanalysis 2 (1990) 303–308, https://doi.org/10.1002/elan.1140020407.

[29] U. Wollenberger, J. Wang, M. Ozsoz, E. Gonzalez-Romero, F. Scheller, Bulk modified enzyme electrodes for reagentless detection of peroxides, Bioelectrochem. Bioenerg. 26 (1991) 287–296, https://doi.org/10.1016/0302-4598(91)80030-7.

[30] A. Morales, F. Céspedes, J. Mũnoz, E. Martínez-Fábregas, S. Alegret, Hydrogen peroxide amperometric biosensor based on a peroxidase-graphite-epoxy biocomposite, Anal. Chim. Acta 332 (1996) 131–138, https://doi.org/10.1016/0003-2670(96)82793-0.

[31] Y. Xiao, H.-X.X. Ju, H.-Y.Y. Chen, Hydrogen peroxide sensor based on horseradish peroxidase-labeled Au colloids immobilized on gold electrode surface by cysteamine monolayer, Anal. Chim. Acta 391 (1999) 73–82, https://doi.org/10.1016/S0003-2670(99)00196-8.

[32] S.-Q. Liu, H.-X. Ju, Renewable reagentless hydrogen peroxide sensor based on direct electron transfer of horseradish peroxidase immobilized on colloidal gold-modified electrode, Anal. Biochem. 307 (2002) 110–116, https://doi.org/10.1016/S0003-2697(02)00014-3.

[33] H. Yin, S. Ai, W. Shi, L. Zhu, A novel hydrogen peroxide biosensor based on horseradish peroxidase immobilized on gold nanoparticles–silk fibroin modified glassy carbon electrode and direct electrochemistry of horseradish peroxidase, Sensor. Actuator. B Chem. 137 (2009) 747–753, https://doi.org/10.1016/J.SNB.2008.12.046.

[34] X. Yi, J. Huang-Xian, C. Hong-Yuan, Direct electrochemistry of horseradish peroxidase immobilized on a colloid/cysteamine-modified gold electrode, Anal. Biochem. 278 (2000) 22–28, https://doi.org/10.1006/ABIO.1999.4360.

[35] L. Menten, M.I. Michaelis, Die kinetik der invertinwirkung, Biochem. Z. 49 (1913) 5.

[36] H. Lineweaver, D. Burk, The determination of enzyme dissociation constants, J. Am. Chem. Soc. 56 (1934) 658–666.

[37] K.R. Brown, D.G. Walter, M.J. Natan, Seeding of colloidal Au nanoparticle solutions. 2. Improved control of particle size and shape, Chem. Mater. 12 (2000) 306–313, https://doi.org/10.1021/cm980065p.

[38] S. Bharathi, M. Nogami, S. Ikeda, Layer by layer self-assembly of thin films of metal hexacyanoferrate multilayers, Langmuir 17 (2001) 7468–7471, https://doi.org/10.1021/la011053c.

[39] B. Neiman, E. Grushka, O. Lev, Use of gold nanoparticles to enhance capillary electrophoresis, Anal. Chem. 73 (2001) 5220–5227, https://doi.org/10.1021/ac0104375.

[40] X. Hua, H.L. Xia, Y.T. Long, Revisiting a classical redox process on a gold electrode by operando ToF-SIMS: where does the gold go? Chem. Sci. 10 (2019) 6215–6219, https://doi.org/10.1039/c9sc00956f.

[41] J. Zhao, R.W. Henkens, J. Stonehuerner, J.P. O'Daly, A.L. Crumbliss, Direct electron transfer at horseradish peroxidase-colloidal gold modified electrodes, J. Electroanal. Chem. 327 (1992) 109–119, https://doi.org/10.1016/0022-0728(92)80140-Y.

[42] X. Li, J. Wu, N. Gao, G. Shen, R. Yu, Electrochemical performance of l-cysteine-goldparticle nanocomposite electrode interface as applied to preparation of mediator-free enzymatic biosensors, Sensor. Actuator. B Chem. 117 (2006) 35–42, https://doi.org/10.1016/j.snb.2005.10.044.

[43] S.H. Jung, J.W. Yeon, K. Song, Effect of pH, temperature, and H2O2 on the electrochemical oxidation behavior of iron in perchlorate solutions, J. Solid State Electrochem. 18 (2014) 333–339, https://doi.org/10.1007/s10008-013-2357-z.

[44] D.C. Harris, Quantitative Chemical Analysis, seventh ed., W.H. Freeman, New York, 2007.

[45] J.W. Mandler, A.C. Stalker, S.T. Croney, D.W. Akers, N.K. Bihl, L.S. Loret, T.E. Young, In-plant Source Term Measurements at Prairie Island Nuclear Generating Station, US Nuclear Regulatory Commission, United States, 1985.

[46] M.G. Garguilo, Nhan Huynh, A. Proctor, A.C. Michael, Amperometric sensors for peroxide, choline, and acetylcholine based on electron transfer between horseradish peroxidase and a redox polymer, Anal. Chem. 65 (1993) 523–528, https://doi.org/10.1021/ac00053a007.

[47] J. Li, S.N. Tan, H. Ge, Silica sol-gel immobilized amperometric biosensor for hydrogen peroxide, Anal. Chim. Acta 335 (1996) 137–145, https://doi.org/10.1016/S0003-2670(96)00337-6.

[48] A.L. Lehninger, D.L. Nelson, M.M. Cox, Lehninger Principles of Biochemistry, fourth ed., W. H. Freeman, New York, 2005.

[49] F. Wu, Z. Hu, J. Xu, Y. Tian, L. Wang, Y. Xian, L. Jin, Immobilization of horseradish peroxidase on self-assembled (3-mercaptopropyl)trimethoxysilane film: characterization, direct electrochemistry, redox thermodynamics and biosensing, Electrochim. Acta 53 (2008) 8238–8244, https://doi.org/10.1016/J.ELECTACTA.2008.06.031.

[50] R.A. Kamin, G.S. Wilson, Rotating ring-disk enzyme electrode for biocatalysis kinetic studies and characterization of the immobilized enzyme layer, Anal. Chem. 52 (1980) 1198–1205, https://doi.org/10.1021/ac50058a010.